Research and design of a waveguide sum-difference comparator for monopulse radar applications

Luu Duc Tho*, Ha Huy Dung, Luong Van Trinh, Cao Viet Linh,
Doan Van Tung, Nguyen Duc Thanh

Institute of Defence Equipment, Academy of Military Science and Technology, 17 Hoang Sam, Nghia Do, Hanoi, Vietnam.
*Corresponding author: luuductho1991@gmail.com
Received 26 Jan. 2026; Revised 13 Mar. 2026; Accepted 13 Mar. 2026; Published 25 Apr. 2026.
DOI: https://doi.org/10.54939/1859-1043.j.mst.110.2026.55-62

ABSTRACT

This paper presents the research and design results of a waveguide sum-difference comparator for monopulse radar applications. The proposed sum-difference comparator is designed to meet the requirements of wide bandwidth, low insertion loss, and high port isolation, while maintaining good amplitude and phase balance across the operating frequency band. Ku-band monopulse radar systems demand waveguide combining networks with high stability and low loss to ensure accurate generation of sum and difference signals. Conventional waveguide T-junction–based comparators are typically limited in bandwidth and exhibit insufficient port isolation, which can degrade monopulse tracking performance. In this work, a Ku-band 4×4 waveguide power combining and dividing network based on a hybrid configuration of H-plane and E-plane slot couplers is proposed for monopulse radar applications. The H-plane slot couplers are employed to achieve in-phase power combining, while the E-plane slot couplers provide phase inversion and enhanced port isolation. Full-wave electromagnetic simulations are carried out using the CST Studio Suite to optimize the geometrical parameters and ensure compliance with the design specifications. The proposed design offers a compact, robust, and high-power-handling solution suitable for Ku-band monopulse radar front-end processing systems.

Keywords: Monopulse radar; Sum–difference comparator; Waveguide; E-plane slot coupler; H-plane slot coupler.

1. INTRODUCTION

Monopulse radar has been widely employed in tracking, navigation, and surveillance systems due to its ability to provide high angular accuracy using a single transmitted pulse. Unlike sequential beam-scanning techniques, monopulse radar determines the target angular error by simultaneously comparing the amplitude and phase of the sum (Σ) and difference (Δ) signals, thereby reducing sensitivity to target echo amplitude fluctuations. Consequently, the performance of a monopulse radar system is strongly dependent on the accuracy, stability, and symmetry of the radio-frequency combining network placed immediately after the antenna or antenna subarrays. The microwave front-end of monopulse radar systems typically operates under high peak power conditions while still requiring low transmission loss and high phase stability. To date, numerous power combining and dividing techniques have been reported in the literature. Various techniques have been reported for implementing microwave power combining and dividing networks, including waveguide structures, microstrip or substrate integrated waveguide (SIW) technologies, monolithic and hybrid microwave integrated circuits (MMIC/HHMIC), and multilayer circuit implementations. SIW-based approaches [1-3] provide compact structures and ease of integration; however, they generally suffer from relatively high transmission loss and limited power-handling capability. MMIC and HHMIC solutions [4-5] offer high integration density and wide bandwidth, but their applicability in high-power radar front ends is constrained by power limitations. Multilayer printed circuit implementations [6] can reduce the overall size, yet they also exhibit

considerable loss and insufficient power capacity for monopulse radar systems. In contrast, waveguide-based networks inherently provide low insertion loss and excellent high-power capability, making them more suitable for radar applications. Previous studies have investigated 2×2 waveguide combiners [7–9]; nevertheless, these designs are difficult to extend to multiport architectures required by practical monopulse systems. Magic-T based structures reported in [10] can generate well-defined sum and difference channels with good port isolation, but their complicated geometry and strict fabrication tolerances significantly limit practical implementation. More recently, 4×4 waveguide combining networks were presented in [11-12]; although these designs enable multiport functionality, their structural complexity and large physical size remain major drawbacks. To overcome these limitations, this paper proposes a compact 4×4 waveguide power combining and dividing network based on a hybrid configuration of H-plane and E-plane slot couplers. In the proposed design, H-plane slot couplers are utilized to achieve low-loss in-phase power combining, while E-plane slot couplers introduce controlled phase inversion and improve signal-path isolation. Compared with previously reported structures, the proposed network simultaneously achieves simplified topology, reduced size, and improved practicality, while maintaining high power-handling capability, wide bandwidth, high port isolation, and favorable transmission characteristics. These features make the proposed structure particularly suitable for modern monopulse radar systems.

2. PROBLEMS

2.1. Overview of waveguide slot coupling techniques

Slot coupling is one of the most widely used power-coupling techniques in microwave systems, particularly in rectangular waveguide structures. The fundamental principle of slot coupling is based on introducing one or more narrow slots in the metallic wall of a waveguide in order to exploit the electromagnetic interaction between the propagating fields in adjacent waveguides. For the dominant TE_{10} mode, the electric and magnetic field distributions inside the waveguide are well defined. Placing coupling slots at locations where the electric or magnetic fields reach their maxima enables effective control of the coupling level, phase relationship, and bandwidth characteristics of the coupled structure. The key geometrical parameters of the slot include its length, width, shape, and position along the direction of wave propagation.

Slot coupling of rectangular guides, E-plane

A junction of two contiguous rectangular guides of equal dimensions coupled on their broad sides by a slot in a wall of zero thickness. Sides of slot perpendicular to the electric field (H_{10} - modes in rectangular guides). The overall configuration and equivalent circuit of the H-plane slot coupler are illustrated in Figure 1.

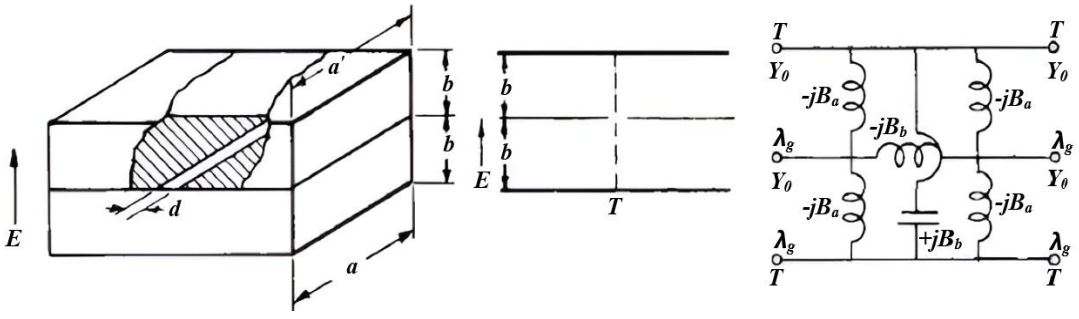

a) General view. *b) Top view.* *c) Equivalent circuit.*

Figure 1. *E-plane slot coupling in a rectangular waveguide.*

Equivalent-circuit parameters at the common reference plane *T*.

$$\frac{B_a}{Y_0}=\frac{\dfrac{2b}{\lambda_g}\left[\dfrac{J_1\left(\pi d/\lambda_g\right)}{2b/\lambda_g}\right]}{1-\dfrac{3}{4}\left(\dfrac{\pi d}{2\lambda_g}\right)^2+\left(\dfrac{\pi d}{2\lambda_g}\right)^2\ln\dfrac{4b}{\pi d}+\dfrac{1}{6}\left(\dfrac{\pi d}{4b}\right)^2-2\left(\dfrac{\pi d}{4b}\right)^2\sum_1\left(\dfrac{2b}{\lambda_g}\right)} \tag{1}$$

$$\frac{B_b}{Y_0}-\frac{B_a}{Y_0}=\frac{4b/\lambda_g}{\left[J_0\left(\pi d/\lambda_g\right)\right]^2}\left\{\left[1-\left(\frac{\pi d}{2\lambda_g}\right)^2\right]\ln\frac{4b}{\pi d}+\sum_0\left(\frac{2b}{\lambda_g}\right)+\frac{1}{2}\left(\frac{\pi d}{2\lambda_g}\right)^2-\frac{1}{6}\left(\frac{\pi d}{4b}\right)^2+2\left(\frac{\pi d}{4b}\right)^2\sum_1\left(\frac{2b}{\lambda_g}\right)\right\} \tag{2}$$

where, $\sum_0(x)=\sum_{n=1}^{\infty}\left(\dfrac{1}{\sqrt{n^2-x^2}}-\dfrac{1}{n}\right)\approx\dfrac{1}{\sqrt{1-x^2}}-1+0.1010x^2+0.0138x^4+\ldots;$

$\sum_1(x)=\sum_{n=1}^{\infty}\left(\sqrt{n^2-x^2}-n+\dfrac{x^2}{2n}\right)\approx\sqrt{1-x^2}-1+\dfrac{x^2}{2}-0.0253x^4;$

a,a',b,b' - waveguide dimensions; d - coupling slot width; λ_g - guide wavelength.

Slot coupling of rectangular guides, H-plane

A junction of two contiguous rectangular guides of equal heights coupled on their narrow sides by a slot in a wall of zero thickness. Sides of slot parallel to electric field (H_{10} - modes in rectangular guides). The overall configuration and equivalent circuit of the H-plane slot coupler are illustrated in Figure 2.

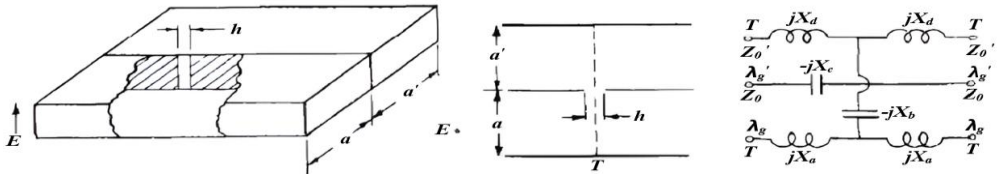

a) General view; *b) Top view;* *c) Equivalent circuit.*

Figure 2. *H-plane slot coupling in a rectangular waveguide.*

Equivalent-circuit Parameters at the common reference plane *T*.

$$\frac{X_a}{Z_0}=\frac{\dfrac{a}{\lambda_g}\left(\dfrac{\pi h}{4a}\right)^4\left(1+\dfrac{a^3}{a'^3}\right)}{1-\dfrac{1}{2}\left(\dfrac{\pi h}{4a}\right)^4\left(1+\dfrac{a^4}{a'^4}\right)},\quad \frac{X_b}{Z_0}=\frac{a}{\lambda_g}\left[\left(\frac{4a}{\pi h}\right)^2+\left(1+\frac{a^2}{a'^2}\right)\right] \tag{3}$$

$$\frac{X_c}{Z_0}=\frac{X_a}{Z_0}\frac{2}{1+\dfrac{a^3}{a'^3}},\quad \frac{X_d}{Z_0}=\frac{X_a}{Z_0}\frac{a^3}{a'^3},\quad \frac{Z_0'}{Z_0}=\frac{\lambda_g'}{\lambda_g}\frac{a}{a'} \tag{4}$$

where, h - coupling slot width; λ_g' - guide wavelength.

2.2. Hybrid E-plane and H-plane slot-coupled structure

In modern microwave and monopulse radar systems, the requirements for accurate power combining and dividing, strict amplitude and phase balance, as well as high power-handling capability and long-term stability, pose significant challenges in the selection and design of coupling structures. When used individually, E-plane and H-plane slot couplers can only partially satisfy these requirements: H-plane slot couplers provide in-phase power division with low insertion loss and wide bandwidth, whereas E-plane slot couplers offer an inherent advantage in

generating the phase inversion required for difference channels.

On this basis, a hybrid E-H plane slot-coupled structure, illustrated in Figure 3, is proposed as an effective solution to combine the advantages of both coupling mechanisms. By appropriately arranging H-plane and E-plane slot couplers within a single waveguide network, in-phase power combining/dividing and controlled phase inversion can be simultaneously realized in a compact configuration, while satisfying stringent requirements on amplitude balance, phase accuracy, and port-to-port isolation.

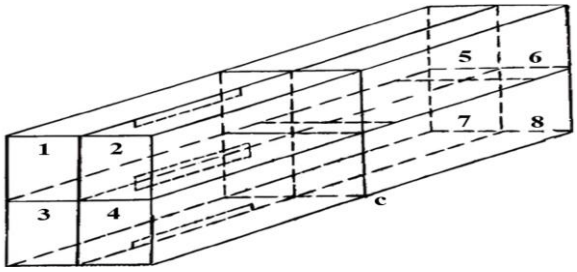

Figure 3. *Proposed structure of the E-H plane slot coupler.*

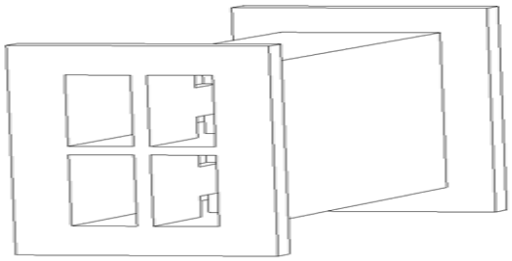

Figure 4. *3D model of the waveguide sum-difference comparator in CST.*

The proposed structure consists of eight ports, including four input ports (Ports 1–4) and four output ports (Ports 5–8). All output ports are connected to waveguide impedance transformers to ensure proper matching with standard waveguides for measurement purposes. Port 7 provides the sum signal, denoted as Σ. Ports 5 and 8 deliver the elevation difference signal Δ_{el} and the azimuth difference signal Δ_{az}, respectively, which are essential for target tracking in monopulse radar systems. Port 6 is terminated with a matched load. In waveguide sum-difference comparators for monopulse radar systems, the transmission amplitude of the sum channel is typically about 3 dB higher than that of the difference channel. This disparity arises from the fundamental principle of electromagnetic field addition and subtraction, the different coupling characteristics associated with the E-plane and H-plane in waveguide junctions, as well as the requirement to ensure a high signal-to-noise ratio for the sum channel in order to improve the accuracy and stability of monopulse angle measurements. The non-uniform power distribution between the two channels is therefore an intentional design choice, optimized for angular processing in modern monopulse radar systems.

The input ports are arranged on one side of the structure, while all output ports are located on the opposite side to facilitate integration with the radiating section of the monopulse antenna system. In addition, the proposed structure can also operate as an equal 4-way waveguide power divider or combiner in the transmit mode, making it suitable for high-power phased-array antenna applications.

The amplitude and phase imbalances among the four receiver channels affect the accuracy of angle measurement. Therefore, the influence of channel imbalance is first analyzed. Here, $f_1(\theta)$, $f_2(\theta)$, $f_3(\theta)$ and $f_4(\theta)$ represent the echo signals arrived at the four antenna sub-array. Each of these signals can be approximated by the expression $\sin\left[k\left(\theta-\theta_{pa}\right)\right]/\left[k\left(\theta-\theta_{pa}\right)\right]$, where k is a constant determined by the antenna half-power point, θ is the angle between the reflected signal and the normal to the antenna plane; $\theta_{pa} \approx 0.4\theta_3$, và θ_3 represent the half-power beamwidth. In an ideal receiver model, the four receiving channels are completely identical; therefore, the analog receiving paths do not introduce angle measurement errors. However, in practice, amplitude and phase imbalances are unavoidable. Hence, it is necessary to analyze the relationship between amplitude and phase imbalances and the resulting angle estimation error. Channel 1 is selected as

the reference channel, and its transfer function is normalized to unity. The transfer functions of the remaining three channels can be expressed as follows: $A_2e^{j\varphi_2}$, $A_3e^{j\varphi_3}$ and $A_4e^{j\varphi_4}$, where, A_2; A_3; A_4 are the amplitude coefficients of channels 2, 3, and 4 with respect to channel 1. The angle measurement errors can be expressed as follows:

$$\text{Elevation angle error: } U_{el} = \text{Re}\left\{\frac{f_1(\theta) + A_2e^{j\varphi_2}f_2(\theta) - A_3e^{j\varphi_3}f_3(\theta) - A_4e^{j\varphi_4}f_4(\theta)}{f_1(\theta) + A_2e^{j\varphi_2}f_2(\theta) + A_3e^{j\varphi_3}f_3(\theta) + A_4e^{j\varphi_4}f_4(\theta)}\right\} \quad (5)$$

$$\text{Azimuth angle error: } U_{az} = \text{Re}\left\{\frac{f_1(\theta) + A_3e^{j\varphi_3}f_3(\theta) - A_2e^{j\varphi_2}f_2(\theta) - A_4e^{j\varphi_4}f_4(\theta)}{f_1(\theta) + A_2e^{j\varphi_2}f_2(\theta) + A_3e^{j\varphi_3}f_3(\theta) + A_4e^{j\varphi_4}f_4(\theta)}\right\} \quad (6)$$

3. RESULTS AND DISCUSSION

3.1. Define design requirements

Based on previously published results in reputable international journals and an examination of several monopulse radar systems, the basic parameter requirements are summarized in table 1. After determining the required technical parameters, the geometric parameters are optimized using full-wave electromagnetic simulation software. Subsequently, a three-dimensional model is constructed in the simulation environment, incorporating the main parameters of the power combining network as listed in Table 2. The three-dimensional model of the proposed sum-difference comparator is illustrated in Figure 4.

Table 1. *Required parameters of the proposed sum-difference comparator.*

№	Techical parameters	Unit	Required value
1	Frequency	GHz	12.5 - 13.0
2	Number of Ports	Ports	4x4
3	Transmission coefficient		
3.1	Sum Channel	dB	6 ± 0.5
3.2	Difference Channel	dB	9 ± 1.5
4	Reflection coefficient	dB	≤ -10
5	Isolation coefficient	dB	≤ -20

Table 2. *Basic dimensional parameters of the proposed sum-difference comparator.*

№	Parameters	Value (mm)	№	Parameters	Value (mm)
1	a	17	4	h	21.7
2	b	8	5	c	70
3	d	7.1			

3.2. Calculation results

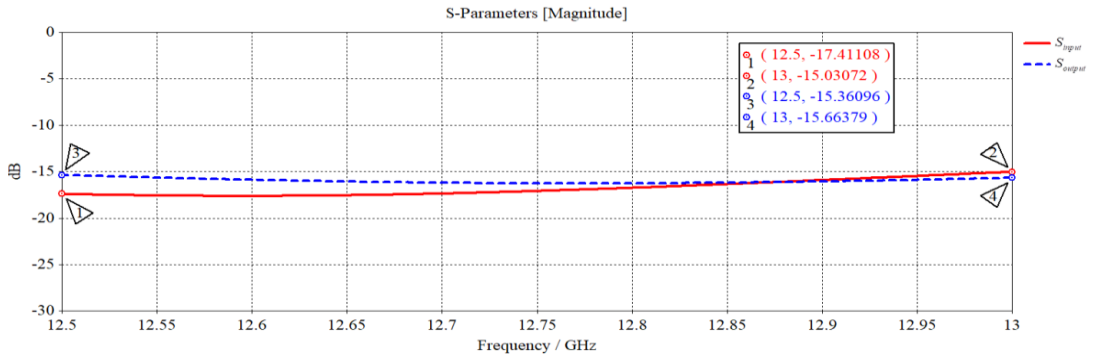

Figure 5. *Reflection coefficient of the sum-difference waveguide comparator.*

After designing and optimizing the parameters using the CST Studio Suite with a time-domain approach, the calculated results of the waveguide sum-difference comparator are presented in Figures 5–7. Figure 5 illustrates the reflection coefficient of the waveguide sum-difference comparator.

The results presented in Figure 5 show that the reflection coefficients at all ports of the coupler are lower than -15 dB over the operating frequency band, indicating good impedance matching characteristics. Figure 6 illustrates the calculated transmission coefficients of the channels of the sum-difference comparator.

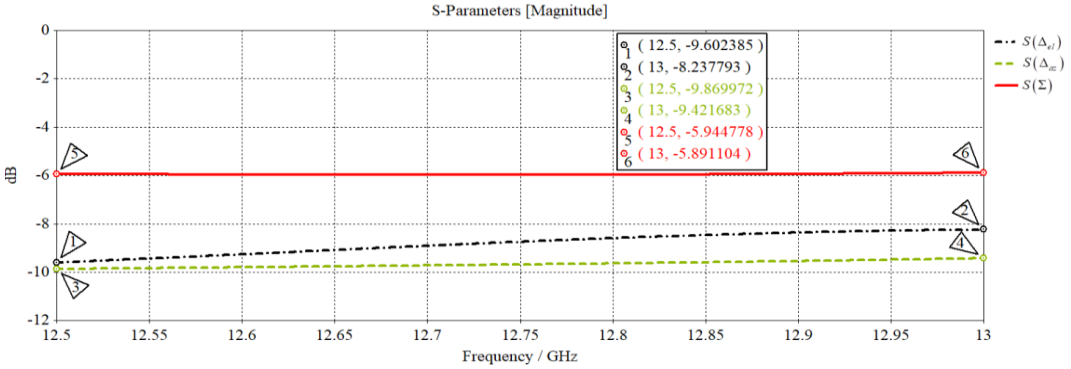

Figure 6. *Transmission coefficient of the sum-difference waveguide comparator.*

The results shown in Figure 6 indicate that the transmission coefficient of the sum channel is (6 ± 0.11) dB, which is lower than that of the difference channels, reaching approximately (9 ± 0.9) dB, thereby reflecting an amplitude discrepancy of about 3 dB between the channels. Figure 7 presents the calculated isolation performance of the sum-difference comparator.

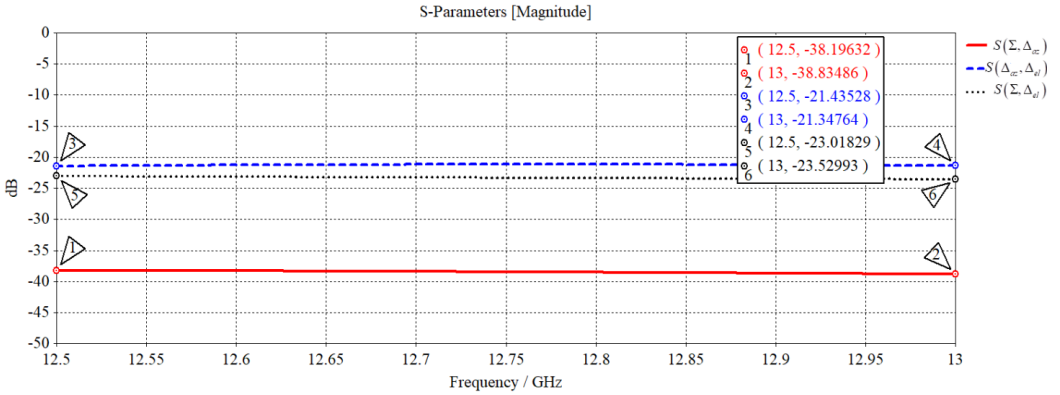

Figure 7. *Isolation coefficient of the sum-difference waveguide comparator.*

Figure 7 shows that the port-to-port isolation of the coupler remains below -21 dB throughout the operating frequency band. The calculated performance of the proposed waveguide sum-difference comparators is summarized in tables 3 and 4 and compared with results reported in the literature.

Table 3. *Waveguide sum-difference comparator calculation results.*

№	Techical parameters	Unit	Required value	Simulation results
1	Frequency	GHz	12.5 - 13.0	12.5 - 13.0
2	Number of ports	Ports	4x4	4x4
3	Transmission coefficient			
3.1	Sum channel	dB	6 ± 0.5	6 ± 0.11
3.2	Difference channel	dB	9 ± 1.5	9 ± 0.9
4	Reflection coefficient	dB	≤ -10	≤ -15.1
5	Isolation coefficient	dB	≤ -20	≤ -21.3

Table 4. *Comparison of the proposed sum-difference comparator with some published types.*

№	Frequency, GHz	Technology	Transmission coefficient, dB	Reflection coefficient, dB	Isolation coefficient, dB
[1]	9.5 - 10.5	SIW (4x4)	7.5 ± 1.5	≤ -10	≤ -20
[2]	14.7 - 15.7	SIW (4x4)	6.02 ± 1	≤ -20	≤ -20
[3]	9.43 - 10.65	SIW (2x2)	3 ± 0.4	≤ -10	≤ -37
[4]	15 - 30	MMIC (2x2)	-	≤ -10	≤ -10
[5]	75 - 79	HHMIC (2x2)	-	≤ -15	≤ -20
[6]	20.5 - 27.8	Multilayer (2x2)	3 ± 1	≤ -10	≤ -20
[7]	56 - 75	Waveguide (2x2)	3 ± 0.5	≤ -20	≤ -20
[8]	17.6 - 23.7	Waveguide (2x2)	3 ± 0.3	≤ -20	≤ -20
[9]	9.57 - 15.33	Waveguide (2x2)	3 ± 0.5	≤ -15	≤ -20
[10]	14.2 - 15.3	Magic T (4x4)	6 ± 0.1	≤ -15	≤ -40
[11]	0.97 - 1.03	Waveguide (4x4)	6 ± 0.8	≤ -10	≤ -40
[12]	9.5 - 10.5	Waveguide (4x4)	-	≤ -20	≤ -20
This work	**12.5 - 13.0**	**Waveguide (4x4)**	**6 ± 0.11**	**≤ -15.1**	**≤ -21.3**

3.3. Analysis of calculation results

The calculated results indicate that the proposed waveguide sum-difference comparator satisfies all the specified technical performance requirements. In addition, a comparative analysis with previously published works in reputable international journals has been presented to further validate the proposed design. The proposed waveguide sum-difference comparator features a compact configuration, making it well suited for radar systems in which size reduction is a critical requirement. Furthermore, the obtained results demonstrate that the proposed structure exhibits stable transmission characteristics, low reflection coefficients, and high port isolation across the operating frequency band, confirming its suitability for practical monopulse radar applications.

4. CONCLUSIONS

This paper has presented an overall study on the analysis and design of a waveguide sum-difference comparator employing a hybrid E-plane and H-plane coupler configuration. By combining theoretical analysis with full-wave electromagnetic simulations carried out in CST, the performance of the proposed structure was evaluated and benchmarked against previously reported results. The obtained simulation results confirm that the proposed waveguide sum-difference comparator meets the stringent technical requirements of monopulse radar systems. These findings serve as a valuable basis for future investigations and the development of high-performance

waveguide sum–difference comparator for monopulse radar applications with progressively higher technical demands.

REFERENCES

[1]. Yi Liu, Hu Yang, Yan He and Jiang Zhu. *"Compact monopulse sum-difference comparator based on double-layer substrate integrated waveguide"*. Electronics letters, (2017).

[2]. R.V. Haro-Baez, J.A. Ruiz-Crus, Juan Corcoles, J.R. Montejo-Garai and J.M. Rebollar. *"A New 4x4 rectangular waveguide short-slot coupler in 3D printed technology at Ku-Band"*. MDPI, (2020).

[3]. Yuanxi Cao and Sen Yan. *"A Dual-mode SIW compact monopulse comparator for sum and difference multi-beam radar"*. IEEE Microwave and wireless components letters, (2021).

[4]. Yang Chen, Yuehang Xu, Liulin Hu, Wei Tong and Ruimin Xu. *"A broad Passive monopulse comparator MMIC"*. IEEE Microwave and wireless components letters, (2017).

[5]. Jaber Moghaddasi and Ke Wu. *"Planar 1800 hybrid coupler with non-interpersed ports for millimeter-wave applications"*. International journal of microwave and wireless technologies, (2019).

[6]. Veljko Napijalo and Brian Kearns. *"Multilayer 1800 coupled line hybrid coupler"*. IEEE transactions on microwave theory and techniques, (2008).

[7]. M. Nasri, D.Zarifi and Uz Zaman. *"A wideband 3-db directional coupler in GGW for use in V-band communication systems"*. IEEE, (2020).

[8]. Ralf Beyer and Uwe Rosenberg. *"Compact top-wall hybrid/coupler design for extreme broad bandwidth applications"*. IEEE, (2005).

[9]. Guendalina Simoncini, Perderico Alimenti and Roberto Vincenti Gatti. *"Single-ridge waveguide compact and wideband hybrid coupler for X/Ku-Band applications"*. MDPI, (2022).

[10]. Jongmin Lee, Changil Choi, Sungmin Noh, Sangpil Lee and Jinho Jeong. *"Compact Ku-Band Monopulse comparator using offset two-step rectangular-prism-based Magic-T"*. IEEE, (2025).

[11]. M. Mohammadi and F.H. Kashani. *"Planar eight port waveguide monopulse comparator"*. Progress in electromagnetics research, (2009).

[12]. Hemant Kumar, Girish Kumar, Yogesh Verma and Prashant Kumar Mishra. *"Compact waveguide monopulse comparator at Ka-band for monopulse tracking"*. IEEE, (2016).

TÓM TẮT

Nghiên cứu, thiết kế bộ ghép tổng-hiệu ống dẫn sóng ứng dụng cho ra đa đơn xung

Bài báo trình bày kết quả nghiên cứu, thiết kế bộ ghép kênh tổng-hiệu ống dẫn sóng ứng dụng cho ra đa đơn xung. Bộ ghép kênh tổng-hiệu được thiết kế nhằm đáp ứng các yêu cầu về dải thông rộng, độ suy hao và độ cách ly tốt, đồng thời đảm bảo được độ đồng đều trong dải tần số hoạt động. Hệ thống radar đơn xung hoạt động trong băng tần Ku yêu cầu mạng ghép sóng dẫn có độ ổn định cao và tổn hao thấp để đảm bảo tạo tín hiệu tổng và hiệu chính xác. Các bộ ghép dựa trên mối nối chữ T sóng dẫn thông thường thường bị hạn chế về băng thông và khả năng cách ly cổng không đầy đủ, điều này có thể làm suy giảm hiệu suất theo dõi đơn xung. Trong bài báo này, một mạng ghép và chia công suất 4×4 ống dẫn sóng băng tần Ku dựa trên cấu hình lai của bộ ghép khe mặt phẳng H và mặt phẳng E được đề xuất cho các ứng dụng ra đa đơn xung. Các bộ ghép khe mặt phẳng H được sử dụng để đạt được sự ghép công suất đồng pha, trong khi các bộ ghép khe mặt phẳng E cung cấp sự đảo pha và cải thiện khả năng cách ly cổng. Các mô phỏng điện từ trường đã được tiến hành trên phần mềm mô phỏng chuyên dụng CST nhằm tối ưu hóa các tham số kích thước, để đả bảo các tham số theo yêu cầu. Kết quả thiết kế được đề xuất cung cấp một giải pháp nhỏ gọn, mạnh mẽ và có khả năng công suất cao cho các hệ thống tiền xử lý radar đơn xung băng tần Ku.

Từ khóa: Ra đa đơn xung; Bộ ghép tổng-hiệu; Ống dẫn sóng; Cầu khe E; Cầu khe H.